Understanding and Controlling the Dielectric Response of Metal–Organic Frameworks

Understanding and Controlling the Dielectric Response of Metal-Organic Frameworks

Matthew R. Ryder,[a] Lorenzo Donà,[b] Jenny G. Vitillo,[b]§ and Bartolomeo Civalleri*[b]

In memory of Roberto Orlando and Claudio M. Zicovich-Wilson

Abstract: Metal-organic framework (MOF) materials have recently been shown to have promising electronic and dielectric properties. This work involves investigating a diverse range of MOFs to rationalise how the different building blocks that form the structure can affect the electronic properties and dielectric response. The analysis, based on quantum mechanical calculations, includes the contribution from the metals involved, the organic linkers and the symmetry and topology of the framework and makes suggestions for future work on low-κ dielectric MOFs. The results confirm that the band gap is primarily due to the electronic levels of the organic linkers and that tuning the band gap can be easily achieved either by linker functionalisation or increasing the aromaticity. The relevance of simple structure-property relationships for different families of isoreticular MOFs via the use of Hammett sigma constants is also highlighted. We have also shown that the polarizability of the framework can be tuned comparably to the band gap. However, the expected low static dielectric constant is less influenced by the composition of the MOF and can be modified by acting on the crystal structure. Indeed, we have shown that it can be directly linked to the framework porosity.

Introduction

Metal-organic frameworks (MOFs) have emerged over the past decade to become one of the most promising classes of porous materials.[1] The diversity of applications being suggested for MOFs is ever-growing with the most significant focus so far being directed towards traditional gas storage, chemical separation (molecular sieving) and catalysis.[2] However, one of the most intrinsically promising aspects of MOF materials is the high level of customisability which allows for their anisotropic structural properties and stability to be tuned and tailored for specific applications.[3] The remarkable versatility in the molecular level design of the materials is made possible by the modular construction of the frameworks. The hybrid structures involve a combination of two primary building blocks: (i) a metal ion or a metal oxide cluster and (ii) an organic linker component to connect the inorganic moieties and form the crystalline structure. This is schematically shown in Figure 1 where the different levels of alteration are illustrated: (i) secondary building units (SBU), (ii) SBUs assemblies and topologies and (iii) framework modifications.

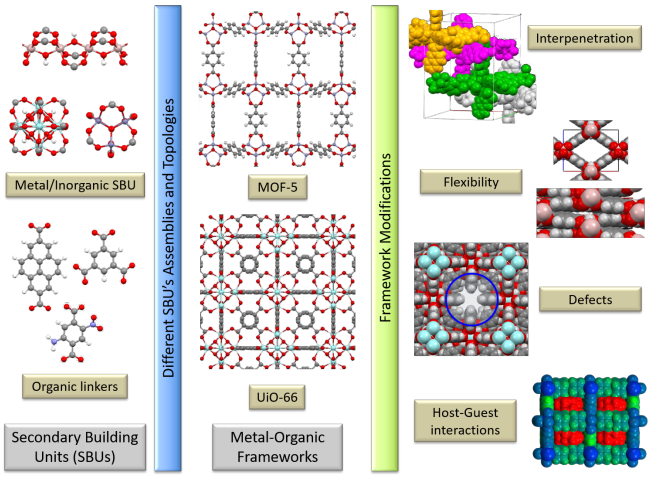

Figure 1. Examples of secondary building units and different assemblies of metal-organic frameworks (MOFs). Modifications of the framework are also highlighted as possible methods to alter response properties. Interpenetration, flexibility (e.g. MIL-53), defects (e.g. missing metal oxide cluster in UiO-66, highlighted in the blue circle) and host-guest interactions (host framework in blue/green and guest in red)

The ability to customise the building blocks has opened many new avenues of research, such as the use of MOFs in optical and microelectronics.[2b, 4] This area of interest is stimulated by the emergence of next-generation photonics, such as optical sensors and switches and requires the introduction of new ultra-low-κ dielectric materials (κ < 1.9) to be used as an interlayer for semiconducting devices.[4a, 5] The International Technology Roadmap for Semiconductors[6] stated that desirable materials should possess a crystalline structure, low density (high porosity), low moisture absorption, and high chemical and thermal stability.[5b] MOFs have also been promoted as future emerging low-κ materials in the "More Moore - White Paper" by the International Roadmap for Devices and Systems.[7]

The current literature has already highlighted the potential of MOFs as low-κ dielectric materials.[8] Theoretical work in the

[a] Dr M.R. Ryder
Department of Engineering Science
University of Oxford
Parks Road, Oxford, OX1 3PJ, United Kingdom

[b] Mr L. Donà, Dr J.G. Vitillo, and Prof. B. Civalleri*
Department of Chemistry
University of Turin
Via Pietro Giuria 7, 10125 Torino, Italy
*bartolomeo.civalleri@unito.it

§ Present address: Department of Chemistry, University of Minnesota, 207 Pleasant Street S.E., Minneapolis, MN 55455-0431

Supporting information for this article is given via a link at the end of the document.

field initially involved the semi-empirical Clausius-Mossotti model, applied to study the dielectric response of cubic Zn-based frameworks.[8] There have also more recently been some *ab initio* studies on similar cubic frameworks and the complex dynamic dielectric constant in the near-ultraviolet (UV) region.[9] These theoretical studies encouraged experimental work on thin films, involving the use of spectroscopic ellipsometry (SE) to report the dielectric and optical properties of HKUST-1[10] and ZIF-8.[11] This studies confirmed that MOFs are indeed promising candidates as low-κ dielectrics.[12] Some of us also recently reported the experimental and theoretical dynamic dielectric response of a selection of ZIF materials in the infrared (IR) and terahertz (THz) spectral regions.[13]

In the present work, we have analysed approximately 50 different MOF structures (see Supporting Information (SI) for the full list), to compare and contrast the effect of different carboxylate linkers and metals. Density functional theory (DFT) calculations allowed us to rationalise the structural and chemical characteristics that can influence the electronic and dielectric properties. The accuracy and computational affordability of DFT and, in particular, of hybrid functionals in predicting electronic and dielectric properties of MOFs (e.g. B3LYP-D*, see Experimental section) have been confirmed by direct comparison with published experimental values where available. Therefore, we aim to provide a guide for those interested in obtaining such electronic and dielectric properties in MOFs.

We confirm that the electronic properties (band gap and polarisability) of these materials can be tuned by either modifying the organic linker (through either functionalisation or expansion, see for instance Figure 2)[14], exchanging the metal ion in the framework,[15] or altering the inorganic moiety with the same organic linker (modifying the framework topology). Tuning the electronic structure of MOFs has recently been discussed in detail by Walsh *et al*.[16] and we aim to extend this interest by investigating how modulating the framework can affect the dielectric response (polarizability, electric susceptibility and dielectric constant).

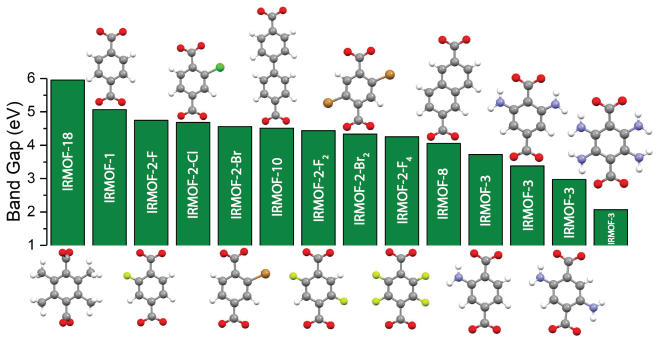

Figure 2. The effect of varying the organic linker on the electronic band gap of the IRMOF-1 family. Colour code: carbon (grey), nitrogen (violet), oxygen (red), hydrogen (white), fluorine (lime green), chlorine (green), bromine (brown).

Results and Discussion

We intend to provide a systematic study of the contributing factors to the low-κ dielectric response and discuss the role of the different structural motifs that comprise the MOF structure, namely: (i) the organic linker, (ii) the metal, and (iii) the framework. We also discuss the role played by framework topology, interpenetration and flexibility (deformation). The effect on the dielectric response due to framework modifications such as defects and host-guest interactions are out of the scope of the present work. However, the effect of such modifications on the structural and electronic properties has been previously reported.[17]

Role of the Linker: IRMOF-1 Family

MOF-5 (hereafter denoted as IRMOF-1) is the first representative framework of an isoreticular series. It was shown by some of us that the top of the valence band and the lowest conduction band are dominated by the contribution of the benzene-1,4-dicarboxylate (BDC) linkers and that the electronic levels of the metal nodes (Zn_4O clusters) did not contribute significantly.[18] The preliminary *ab initio* calculations suggested that the band gap of isoreticular frameworks related to MOF-5 could be tailored and engineered to have specific values by modifying only the organic linker.

We expand upon the work discussed above by considering a significantly larger series of IRMOFs and investigating a variety of different organic linkers including both functionalised and extended IRMOF systems. The IRMOFs discussed have primarily been reported by Eddaoudi *et al*.,[14b] Gascon *et al*.,[19] and Meek *et al*.[20] In particular, the functionalised IRMOFs studied are: (i) the halogenated IRMOF-2-X series (X = F, Cl, Br) with mono-, di- and tetra-substituted terephthalate linkers (2-, 2,5- and 2,3,5,6-tetra); (ii) the amino substituted IRMOF-3 series ($BDC\text{-}NH_2$) with mono-, di- and tetra-substituted linkers (2-, 2,5-di-, 2,6-di- and 2,3,5,6-tetra); (iii) the tetramethyl-substituted IRMOF-18. IRMOFs with 2-nitrobenzene-1,4-dicarboxylate ($IRMOF\text{-}1\text{-}NO_2$) and a mixed amino and nitro functionalized terephthalic acid linker (IRMOF-1-AN) were also both studied as well. The latter was included in designing a linker like that of push-pull organic molecules, where the band energies are influenced primarily by the electron-donating or withdrawing capability of substituents present. With regards to the extended IRMOFs, they include: (i) naphthalene-2,6-dicarboxylate (IRMOF-8); (ii) biphenyl (IRMOF-10); (iii) 4,5,9,10-tetrahydropyrene-2,7-dicarboxylate (IRMOF-12); (iv) pyrene-2,7-dicarboxylate (IRMOF-14). Finally, we included interpenetrated structures of IRMOF-1 (IRMOF-1-IP) and IRMOF-10 (known as IRMOF-9) to examine the effect of framework interpenetration. Some of the organic linkers are shown in Figure 2 along with the electronic band gap in the corresponding IRMOF.

The comparison between the computed band gaps and the available experimental values reported by Gascon *et al*.[19] is shown in Figure 3. It is well known that the B3LYP DFT functional slightly overestimates the band gap (see Experimental section). However, the comparison between the B3LYP-D* results and the experimental data reported in Ref. [19] shows the same difference between the framework structures and is reasonably good considering the error margin of the synthetic procedure (concentration, temperature, and post-synthetic treatment).[21] It is also encouraging to see that the overestimation (approximately 15%) in the predicted values is systematic therefore confirming that the hybrid B3LYP-D* functional can be used to predict the band gaps of the full set of IRMOFs.

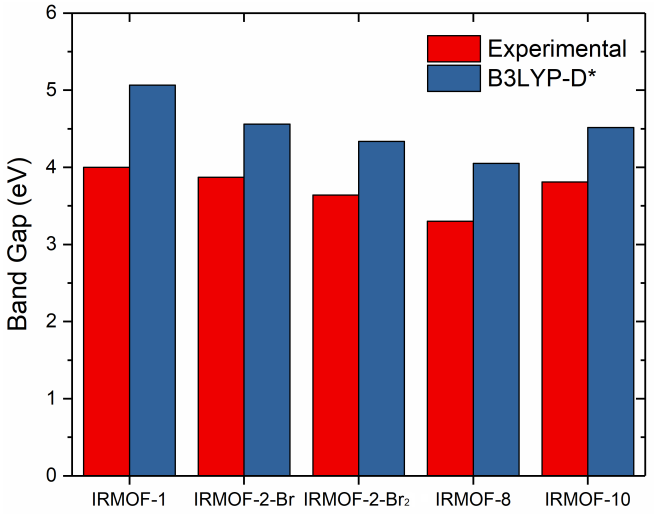

Figure 3. Comparison between the experimental values in Ref. [19] (red bars) and the computed band gaps (blue bars) using the B3LYP-D* DFT functional for selected IRMOFs.

The computed polarizabilities, band gaps and static dielectric properties of the IRMOFs discussed here are reported in Table 1. For the IRMOF-2-X structures, the effect of systematically increasing the halide substituents was studied, and the fluorination example is shown in Figure 4. This was to understand the impact on the band gap and polarizability from replacing one or more of the hydrogen atoms with fluorine and hence allowing the cavity of the framework to become increasingly hydrophobic. The motivation to increase the hydrophobicity of the pore structure is to reduce the likelihood of water molecules adsorbing into the framework. Water has a higher dielectric constant than a vacuum, so its adsorption must be avoided to maintain the low-κ dielectric response. Also, the presence of fluorine can improve the framework stability by reducing degradation resulting from water adsorption. We recently reported that the framework porosity has a direct relationship with the static dielectric constant (also later confirmed in this work) and hence to obtain desirable low-κ dielectric constants the porosity should be maximised.[13] Fluorine has a relatively small atomic radius (compared to other halides), so it does not reduce the framework porosity significantly, and the dielectric constant is reasonably unaffected.

The effect of increasing the level of fluorination appears to be systematic with increasing polarizability and a decreasing band gap upon additional fluorine group substitution (Figure 4). A similar response is witnessed for other halide substitution (chlorine and bromine, see Table 1). However, of significant interest is that the dielectric constant is virtually unaffected by fluorination with the value remaining at ~1.37 for all four structures. Any small numerical changes are linked to the slight change in porosity due to the increased size of a fluorine atom compared to hydrogen, and this is confirmed by the increased change witnessed when adding bromine groups (an increase in the dielectric constant by ~0.05 per bromine substitution). This is because of the bulkier bromine atoms, compared to hydrogen (and fluorine).

Table 1. Band gap values (in eV), polarizabilities per unit cell, α (in Å^3) and dielectric tensor, κ, computed with the B3LYP-D* functional. Structures are ordered by increasing polarizability.

IRMOF	Band gap (eV)	α (Å^3)	κ
IRMOF-1	5.07	868.2	1.37
IRMOF-2-F	4.75	871.2	1.37
IRMOF-2-F$_2$[a]	4.44	876.9	1.37
IRMOF-2-F$_4$	4.25	883.8	1.37
IRMOF-2-Cl[a]	4.68	947.3	1.40
IRMOF-3-(NH$_2$)[a]	3.72	958.2	1.41
IRMOF-1-(NO$_2$)	4.82	965.0	1.41
IRMOF-2-Br	4.56	999.3	1.43
IRMOF-3-(NH$_2$)$_2$[a]	3.38	1031.1	1.43
IRMOF-1-AN	3.87	1083.1	1.46
IRMOF-2 Br$_2$[a]	4.34	1134.9	1.48
IRMOF-18	5.95	1175.2	1.50
IRMOF-3-(NH$_2$)$_4$	2.07	1244.6	1.51
IRMOF-8[a][b]	4.05	1162.4	1.31
		1446.4	1.39
IRMOF-10	4.51	1408.3	1.25
IRMOF-12	4.07	1721.4	1.31
IRMOF-1-IP[a][b]	4.86	1825.5	1.77
		1795.8	1.76
IRMOF-14	3.63	1831.5	1.33
IRMOF-9[a][b]	4.46	2676.4	1.48
		2991.4	1.54

[a] Non-cubic space group. XY component of the dielectric tensor below -0.012, otherwise [b] indicates that the first and second rows refer to XX and ZZ components of the dielectric tensor, respectively. IP: interpenetrated.

The predicted band gaps of the IRMOFs can be rationalised by using relationships such as Hammett sigma constants.[22] In Figure 5, the correlation between the magnitude of the band gap and the sigma parameters σ^0_R and σ_I is shown for the substituted IRMOFs. σ^0_R is a descriptor of the resonance effects (a measure of the ability to delocalize π-electrons) while σ_I represents the field-effect (electrostatics). The correlation between the band gap and σ^0_R was proposed by Gascon *et al*. by experimental UV/Vis measurements for a selection of IRMOFs.[19] Here, we confirm that such a correlation is also valid on a theoretical basis and importantly holds for a much more extensive and comprehensive set of structures. The agreement between experiment and theory for the resonance effect is very good. Also, for the first time, we include the correlation between the band gap and σ_I. However, for field effects, the relationship

with the band gap is much less remarkable than for resonance effects. Nevertheless, the band gap of the amino-group containing IRMOF-3 structures reduces significantly with σ_I when increasing the number of substituents on the aromatic linker (highlighted in Figure 5b). The change in the field effect for the IRMOF-3 structures is due to the formation of hydrogen bonds between the hydrogen atoms of the amino groups and the oxygen atoms of the carboxylates and hence results in a more substantial delocalisation of the π-electrons. Therefore, the combination of both the resonance and field effects is likely the reason for the very low band gap of the fully amino-substituted IRMOF-3 structure. Worth noting is that qualitatively the impact of amino-group substitution on the dielectric constant is the same as for the halide substitution, whereby the dielectric constant only increases slightly due to the steric bulk of the substituent. For the amino-groups, this is approximately 0.03-0.04 per replacement. Long *et al*. showed experimentally that amino-group functionalisation could be used to lower the electronic band gap of UiO-66, a Zr-based MOF discussed later in this work.[23] This was also confirmed by Hendon *et al*. for the Ti-based MOF, MIL-125, where they reported that the optical properties could be engineered through ligand functionalisation, with the band gap lowering to 1.28 eV upon double amino-substitution of the BDC linker.[24]

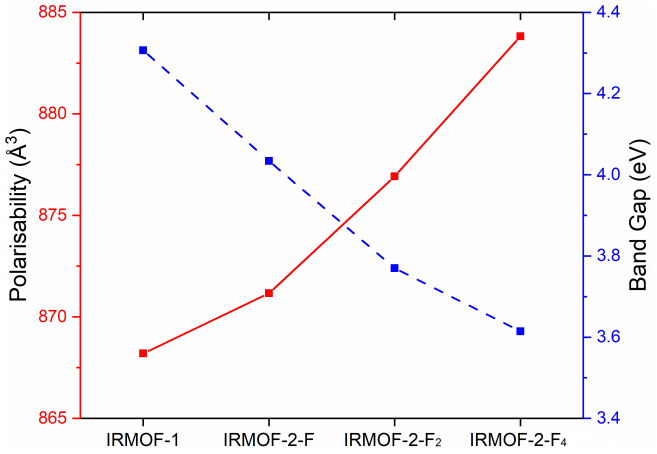

Figure 4. The relationship between the increased fluorination of the aromatic linker and polarizability (solid red) and band gap (dashed blue). Values obtained at the B3LYP-D* level.

Moving on to the IRMOFs with extended linkers, there was no correlation with the Hammett constants when regarding the polarizability or band gap, as would be expected, as the electronic properties are not being changed significantly. However, there was a clear trend between the static dielectric constant and the porosity of the IRMOFs, with the dielectric constants decreasing as the larger extended linkers made the framework increasingly more porous. The lowest dielectric constant was computed for the most porous IRMOF studied, IRMOF-10. This was, in fact, the smallest dielectric response of all the MOFs investigated in this work.

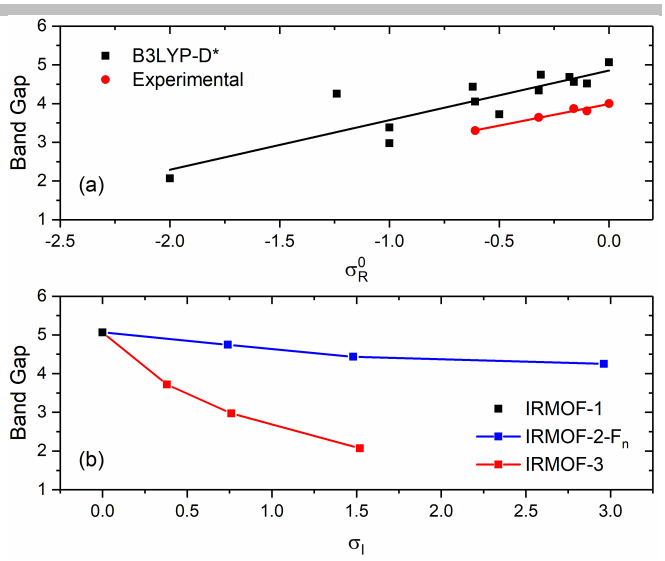

Figure 5. (a) Correlation between calculated values of the band gap and the resonance effect (σ^0_R) for the IRMOF structures, as evidenced by experimental (red filled circles) and computed values (black filled square). (b) Correlation between the band gap and the field effect (σ_I) upon fluorination (blue) and amination (red) in IRMOFs. The value for IRMOF-1 is also reported as a black square.

Therefore, the polarizability and band gap can be controlled by either modifying the linker (halogenation, methylation, amination) or extending it (isoreticular expansion). However, the primary contributing factor to the dielectric constant is merely the level of framework porosity. Interestingly this means that the polarizability and band gap can be changed and modified without significantly affecting the dielectric constant. This is promising, as it allows for modifications such as making the framework voids hydrophobic and therefore more robust in real life applications when water moisture could be detrimental to the low-κ response. Alternatively, it also allows for a low-κ dielectric material with tunable electronic properties.

Role of the Linker: Other Isoreticular Series

To further substantiate the role of the linker, we studied some other topical isoreticular expanded MOF structures, namely: the higher stability UiO and MIL-140 materials which are both Zr-based and have the same organic linkers. The previous section relating to the IRMOFs confirmed that modifying the organic linker could be a powerful way to tailor the band gap and polarizability of the framework. However, another method could be to alter the topology or orientation of the metal clusters. UiO-66 and UiO-67 both have cubic symmetries and possess $Zr_6O_4(OH)_4$ nodes, with the former having 1,4-benzenedicarboxylate (BDC) linkers and the latter being expanded with biphenyl-4,4'-dicarboxylate (BPDC) linkers. The pore geometries present in the UiO structures include an octahedral pore that is face shared with eight smaller tetrahedral ones and edge shared with eight other octahedra.[25] Alternatively, the MIL-140 series are lower in symmetry (monoclinic) and show highly anisotropic mechanical properties.[26] However, instead of isolated $Zr_6O_4(OH)_4$ clusters, as inorganic building blocks, the MIL-140 materials have infinite one dimensional (1D) zirconium oxide (ZrO) chains that are located along the crystallographic *c*-axis (Figure 6). As a result, a distinctive difference in the MIL-140 structures, is the presence

of 1D pore channels along the *c*-axis, resulting in the overall porosity and volume being smaller than for the UiO series.[26c]

Interestingly, we observe a similar response for the Zr-based isoreticular series to that of the IRMOFs discussed above, including the effect of linker substitution (halogenation and amination, see SI). This is promising because of the higher thermal and mechanical stability of the UiO and MIL-140 materials and their lower propensity to form interpenetrated structures (discussed later) compared to the IRMOF series with long organic linkers. However, it is worth noting that their increased stability comes at the cost of framework porosity and hence the dielectric constants of UiO-66 and UiO-67 are 1.90 and 1.63 respectively. Therefore, we also investigated the even further extended member of the series, UiO-68, which has triphenyl-4,4''-dicarboxylate (TPDC) linkers. The mechanical stability of the structure is reduced due to such long (flexible) dicarboxylate linkers, although the dielectric constant lowers to 1.48. This then highlights the need for high stability structures that simultaneously possess prominent levels of framework porosity. Some exciting work has been focused on increasing the mechanical stability of such structures via post-synthetic modification (PSM).[27] However, increasing the stability through brominating the aromatic ring again reduces the porosity as mentioned above and therefore this area of research will be challenging.

A particularly promising alternative could also be MOFs containing tetracarboxylate polyaromatic linkers such as the NU-1000 frameworks.[28] These Zr-based highly porous materials are more robust due to the increased rigidity of the multidentate organic linkers yet due to the significant level of porosity, we compute the static dielectric constant to be 1.38-1.54 (*a*- and *c*-axis due to anisotropy), the lowest of any of the Zr-based MOFs studied.

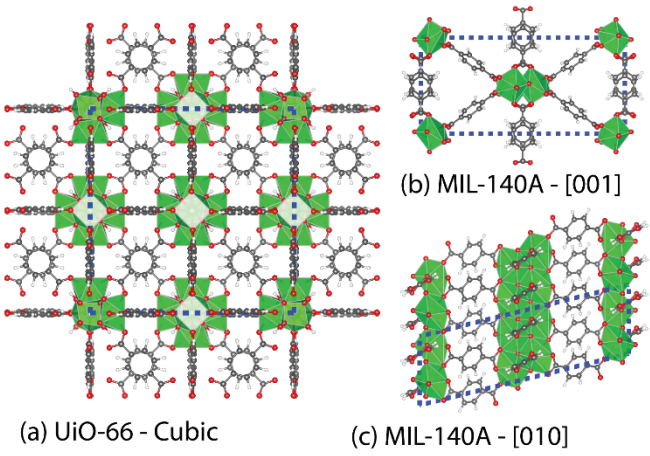

Figure 6. Framework structures of (a) UiO-66 and MIL-140A along the crystallographic (b) *c*-axis and (c) *b*-axis. The inorganic building units are ZrO coordination polyhedra, highlighted in green. Dashed blue lines represent one unit cell. Colour scheme adopted: Zr: green; C: grey; O: red; H: white.

Role of the Metal: MOF-74-M

The MOF-74-M (M = Mg, Mn, Fe, Co, Ni, Zn) frameworks (also known as CPO-27-M) contain one-dimensional channels (Figure 7) which are filled with solvent (e.g. water) that can be removed by mild thermal treatment. Upon dehydration, the crystalline structure is preserved, and a material with a high surface area containing unsaturated metal sites organised in helical chains is obtained.[29] The organic ligands connect each chain with three other adjacent ones which result in the structure's honeycomb motif (Figure 7). The channels in the honeycomb have a diameter of ~11 Å and at the intersections there are helical chains of cis-edge connected metal-oxygen octahedra running along the *c*-axis. All the oxygen atoms of the ligand are involved in the coordination of M^{2+}. These account for five of the oxygen atoms coordinating each metal atom, while the sixth coordinative bond is a solvent molecule which points towards the channel and can be removed upon activation (heating).

The associated band gap values of each of the MOF-74-M structures studied, and of their related metal oxides, are reported in Table 2. All MOF-74-M frameworks have narrow band gaps ranging between 2.8 eV and 3.5 eV. The lowest band gaps are predicted for MOF-74-Fe (2.83 eV) and MOF-74-Ni (2.85 eV), which for the latter is in reasonable agreement with the reported experimental value (MOF-74-Ni: 2.7 eV) obtained from UV/Vis spectroscopy.[30]

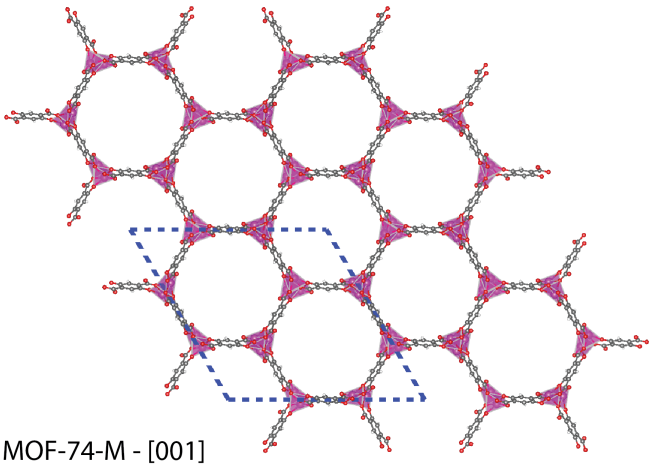

Figure 7. Framework structure of MOF-74-M (M = Mg, Mn, Fe, Co, Ni, Zn) along the crystallographic *c*-axis. The inorganic building units are MO_5 coordination polyhedra, highlighted in pink. Dashed blue lines represent one unit cell. Colour scheme adopted: M: pink; C: grey; O: red; H: white.

Each of the MOF-74-M structures studied demonstrates a much smaller band gap than its related oxide (Table 2). For Zn, the cubic rocksalt-type phase has been used for comparison instead of the most stable wurtzite polymorph due to the comparable octahedral coordination. Interestingly, the most substantial variation in the band gap with respect to the corresponding oxide is observed for Mg, which goes from being an insulator to having a narrow band gap. A similar response has been predicted for the Zr-based MOF, UiO-66, for which the computed band gap decreases significantly with respect to ZrO_2

phases.[31] It is also worth noting that the band structure of every system discussed is almost featureless and shows negligible dispersion of the electronic bands (as shown in Section S6 of the SI for UiO-66 and other selected MOFs).

For closed-shell metals, with valence orbitals fully occupied (Mg and Zn), the band gap is dominated by the electronic levels of the organic linkers (as discussed above). This is comparable to what we previously observed for MOF-5.[18] However, for the other metals with open-shell electronic structures, the band gap is partially influenced by the presence of the unoccupied *d*-orbitals of the metal. This is shown by the lower band gaps predicted where there is a contribution of the *d*-orbitals. The top of the valence band is still dominated by the electronic levels of the linker; therefore, the conduction band represents the largest contribution from the metal orbitals (see Section S6 of the SI for the band structures of MOF-74-Ni). To further substantiate the role of the metal, we also studied the MIL-127 series with other varying tri-valent metals (Al, Sc, Cr, Fe) and witnessed a similar effect on the polarizability and band gap (see Section S4 and S5 of the SI for computed values).

The effect of metal substitution is important for many of the same reasons highlighted for the organic linkers. Due to the dielectric constant being almost exclusively related to the porosity of the system, it allows for the band gap and polarizability to be modified via exchanging the metal without significant alteration to the dielectric response.

Table 2. Band gaps (in eV) for the six MOF-74-M systems and the related metal oxides (in parentheses), along with the polarizabilities per unit cell, α (in Å^3) and dielectric tensor, κ, computed with the B3LYP-D* functional.

Metal	Band Gap (eV)	α (Å^3) (*a*-axis)	α' (Å^3) (*c*-axis)	κ (*a*-axis)	κ' (*c*-axis)
Mg	3.35 (6.90)	459.5	628.5	1.64	1.88
Mn	3.24 (3.04)	578.3	757.6	1.76	1.99
Fe	2.83 (-)	608.9	830.7	1.83	2.13
Co	2.98 (3.18)	615.1	824.5	1.85	2.14
Ni	2.85 (3.99)	612.3	806.9	1.87	2.15
Zn	3.47 (4.22)[a]	541.1	719.8	1.75	1.99

[a] Cubic (rocksalt-type) phase.

Role of Interpenetration and Framework Flexibility

The role of framework interpenetration was studied to extend the investigation to another way of modifying the structure of the material. As reported in Table 1 for IRMOF-1-IP and IRMOF-9, the result is a reduction in the band gap and an increase in the polarizability with respect to the corresponding non-interpenetrated frameworks. Also, as would be expected, the dielectric constant increases due to the decreased pore size. The interpenetrated compounds possess similar unit cell sizes to their non-interpenetrated analogues but with double the density. Therefore, to ensure minimisation of the dielectric constant, it would be advisable to avoid materials that are prone to framework interpenetration.

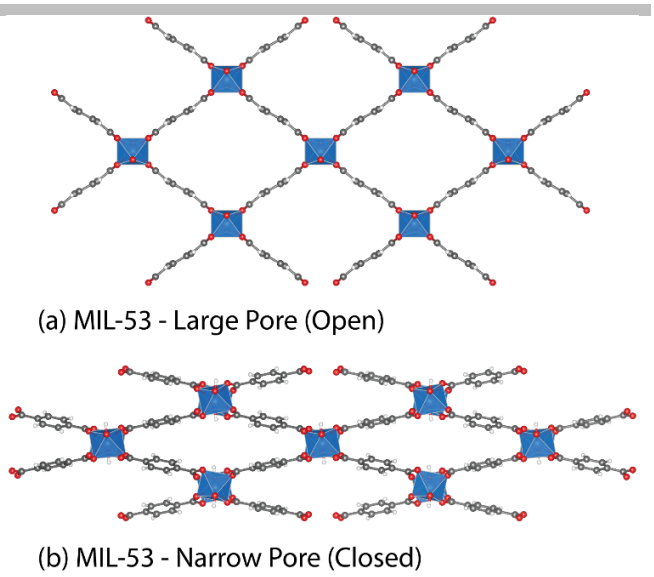

Figure 8. Framework structures of the (a) large pore (open) and (b) narrow pore (closed) geometries of MIL-53. The inorganic building units are AlO_6 coordination polyhedra, highlighted in blue. Colour scheme adopted: Al: blue; C: grey; O: red; H: white.

For completeness, we also studied the effect of phase transformation and flexibility (deformation) of the framework. Soft porous materials such as the MIL-53 structures have been reported to show a substantial band gap change as a result of the open and closed phase transition (Figure 8).[32] MIL-53 is a terephthalic-based MOF that can reversibly switch between an open and closed pore structure upon different stimuli, such as gas pressure or temperature change. Our computed values are consistent with those reported by Ling *et al.*[32a] and show a decrease in the band gap and an increase in the polarizability (along the *a*- and *c*-axes) when going from the open structure (4.85 eV and 331.0/218.2 Å^3) to the non-porous closed phase (3.53 eV and 415.2/372.1 Å^3). As would be expected, there is a significant increase in the dielectric constant for the closed phase as the porosity is removed. However, it is interesting that the dielectric response remains on the same systematic trend as the other structures reported and has an average value of ~2.75 (Figure 9). The reason an average value was used is due to the anisotropic optical properties resulting from the monoclinic symmetry, and therefore the three different dielectric constants were averaged (considering lattice parameter differences). This could imply that for materials such as transition metal-containing MOFs that the framework itself could be somehow limited to a static dielectric constant of approximately 2.75 (linear fit in Figure 9). This is excluding more complex effects such as the diffusion of guest molecules through pore channels, which has been shown to result in large dielectric values at select temperatures.[33] To further clarify whether a dielectric response limit (for empty frameworks) has any merit, we investigated the effect of eliminating the porosity caused by the presence of bulky aromatic groups in the linker. The perfect model structure for this is $Zn(OA)_2$, which is like a MOF but with oxalic acid (OA) as the linkers. OA is the simplest dicarboxylic acid and as some of us have reported previously is highly electrophilic.[34] Therefore, as may be expected we witness very low polarizability and a large band gap. It is, however, encouraging that the resultant dielectric constant, averaged over the three

crystallographic axes (monoclinic symmetry) was consistent, giving a value of ~2.77.

It is important to highlight that the postulated limit for the static dielectric constant of empty MOFs so far holds for transition metal-containing systems. There has recently been some interesting work by Pathak *et al*. that reports the temperature dependent dielectric response of a samarium (Sm)-based MOF.[35] They describe the lanthanide-based framework as a high-κ dielectric material with a dielectric constant of 45.1 (at 5 kHz and 310 K). However, it is worth noting that this material does not contain any hydrocarbon groups, and could, therefore, be expected to behave more like a dense inorganic material.

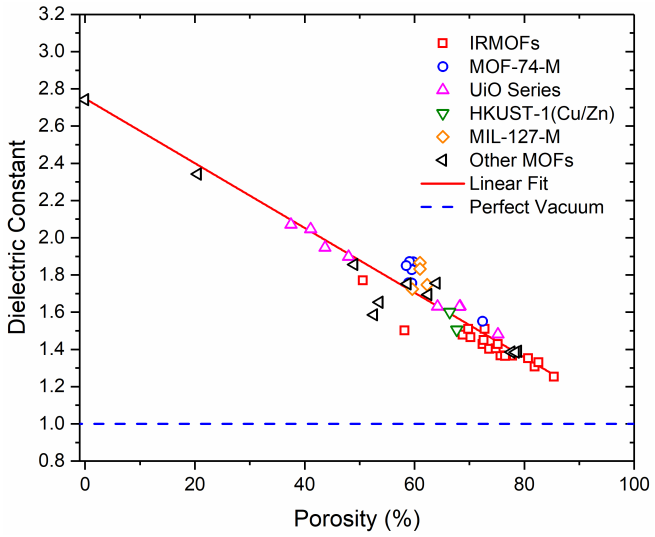

Figure 9. Correlation between the B3LYP-D* static dielectric constant and the framework porosity for all MOFs studied in the present work. A linear fit (R^2 = 0.90) of the data is also reported as a red line to highlight the direct relation between the two properties. The vacuum dielectric constant is shown (blue dashed line) for comparison.

Conclusions

In this work, we have demonstrated that MOFs can be both insulators and have very narrow band gaps (like semiconductors) and possess very low dielectric constants, a combination of remarkable interest for the microelectronics industry.[36] We have predicted with an extensive and diverse selection of MOFs that the value for the static dielectric constant can be below 2.0 and reach as low a value as 1.25 (Figure 9). This highlights MOFs as competitive to traditional low-κ materials such as porous organosilica (κ = 2.4-2.2), aerogels and xerogels (κ < 2.0), periodic nanoporous silicates (e.g zeolites, κ = 2.5-2.0) and periodic mesoporous organosilicas (κ < 2.0).[5b, 37] The broad range of MOF structures explored in this article has allowed us to rationalise the results of the electronic and dielectric response (mostly regarding polarisability) according to the different components that constitute the construction of a MOF (organic linkers and metal nodes) and also the framework structure itself. This then allowed us to verify the relevance of simple structure-property relationships for different families of IRMOFs via the use of Hammett sigma constants as previously proposed through experiments.

We have confirmed that the band gap is mainly due to the electronic levels of the organic linkers and that the tuning of the band gap can be easily achieved either by linker functionalization or increasing the aromaticity. Present results indicate that the larger the delocalisation of the π-electrons of the linker the smaller the band gap. MOFs with larger linkers have been demonstrated to have higher polarizability, and due to the increased porosity, they have lower dielectric constants. Metal substitution affects the band gap only when the electronic levels of the metal are present within the gap. This can be achieved typically for transition metal ions with unpaired electrons (e.g. some of the MOF-74-M frameworks or MIL-125). The presence of open metal sites in MOFs could also be appealing for sensing because the guest interaction with the metal would have a measurable effect on the dielectric response. Indeed, adsorbed molecules (guests) can modulate the electronic structure of the MOFs but would also increase the dielectric constant.

Despite the chemical versatility of MOFs that allows for tuning the band gap and polarizability of the material using different metals and organic linkers, the value of the static dielectric constant is mainly related to the framework. A clear correlation of the dielectric constant with the framework porosity has been found. This would, therefore, suggest that the challenge for having ultra-low-κ dielectrics is to maximise the porosity of the framework while simultaneously maintaining high chemical, mechanical and thermal stability. As a result of our findings due to the mechanical (e.g. bulk and shear modulus, see Supporting Information) and thermal stability of UiO-66, it could be considered as a suitable candidate for further investigation in real applications and devices.[31, 38] We have also highlighted that fluorination could be a robust method to maintain the porosity in real-life situations where water moisture could increase the dielectric constant and affect the material stability.

Several aspects remain open for future investigation such as a full understanding of nonlinear optical properties, through anisotropic porosity and mixed linker systems. The overall effect is predictable but creates a more significant challenge due to the resultant directional mechanical stability of highly anisotropic systems.[26a, 39] Two modifications not covered in this work include (i) host-guest interactions and (ii) defect engineering. For both, the effect would be a modulation of the electronic structure, but in the former, a significant increase of the dielectric constant would be observed due to decreased porosity. The opposite would be expected for defects because of an increase of the porosity due to the presence of defects in the framework. This is an area we are currently investigating. Preliminary results on a model structure of UiO-66 with a missing cluster-defect[40] show that the dielectric constant reduces from 1.90 to 1.73. Another interesting direction would involve investigating the effect of the dielectric response of MOF thin films, such as HKUST-1,[10, 41]

where materials have recently been shown to modify the dielectric layer in field-effect transistors.[41b]

Experimental Section

Contrary to many of the initial studies in the literature on the electronic properties of MOF materials, Local Density Approximation (LDA) and Generalised Gradient Approximation (GGA) have been shown to be inadequate to describe the band gap and dielectric response of solids properly.[42] It has been highlighted that hybrid functionals are required to compute the electronic properties of solids more accurately, and this has recently been confirmed for MOFs.[24] We, therefore, calculated the theoretical static dielectric constants using first-principles DFT and adopted the B3LYP hybrid exchange-correlation functional,[43] with a semi-empirical dispersion correction explicitly developed for solid crystalline systems (B3LYP-D*).[44] All-electron atom-centred Gaussian-type basis sets of at least double-zeta quality were used, as implemented by the periodic *ab initio* CRYSTAL17 code.[45] A full relaxation of both lattice parameters and atomic coordinates was allowed to optimise the geometries of each of the structures. More computational details such as the atomic basis sets, shrinking factors, number of k-points, space group and Laue's class of the investigated MOFs are reported in the Supporting Information (Section S1) along with crystallographic information files (CIFs) of the MOF structures.

The static dielectric constants were then calculated analytically via a Coupled-Perturbed Hartree-Fock/Kohn-Sham (CPHF/CPKS) approach.[46] The CPHF/CPKS method involves computing the polarizability (and dielectric) tensor. The total energy of the material in a constant static field is calculated from the following equation, truncated at the second order, therefore not including the contributions from the hyper-polarizabilities:

$$E(\varepsilon) = E(0) - \sum_t \mu_t \varepsilon_t - \frac{1}{2}\sum_{tu} \alpha_{tu}\varepsilon_t\varepsilon_u - \cdots \quad (1)$$

where E(0) is the field-free energy, ε is the electric field, μ is the dipole moment and α is the polarizability. The dipole moment and the polarizability are related to the energy derivatives according to the following equations (for a much more in-depth explanation see Ref. [42c]):

$$\mu_t = -\frac{\partial E}{\partial \varepsilon_t} \quad (2)$$

$$\alpha_{tu} = -\frac{\partial^2 E}{\partial \varepsilon_t \partial \varepsilon_u} \quad (3)$$

The computed polarizability can then be transformed into the macroscopic first-order susceptibility (χ) from the following equation:

$$\chi_{tu} = \frac{4\pi}{V}\alpha_{tu} \quad (4)$$

where we can see that the susceptibility is strongly affected by the volume of the unit cell (V). The dielectric constant (ε or commonly κ when discussing applications) can then be computed from:

$$\varepsilon_{tu} = \chi_{tu} + \delta_{tu} \quad (5)$$

where δ_{tu} = 0 except when t = u, where δ_{tu} = 1. Hence, in the case of a vacuum when ε = 1, the susceptibility reduces to zero.

Acknowledgements

M. R. R. would like to thank the UK Engineering and Physical Sciences Research Council (EPSRC) for a Doctoral Prize Fellowship and the Rutherford Appleton Laboratory (RAL) for access to the SCARF cluster and additional computing resources. B. C. would like to thank S. Novarino and L. Valenzano for their initial contribution to this work.

Keywords: Metal-Organic Frameworks • Dielectric Properties• Electronic Properties • Density Functional Theory • Porous Materials

[1] H. C. Zhou, J. R. Long, O. M. Yaghi, *Chem. Rev.* **2012**, *112*, 673-674.
[2] aH. Furukawa, K. E. Cordova, M. O'Keeffe, O. M. Yaghi, *Science* **2013**, *341*, 1230444; bM. R. Ryder, J. C. Tan, *Mater. Sci. Technol.* **2014**, *30*, 1598-1612.
[3] A. J. Howarth, Y. Y. Liu, P. Li, Z. Y. Li, T. C. Wang, J. Hupp, O. K. Farha, *Nat. Rev. Mater.* **2016**, *1*, 15018.
[4] aM. Shruti, L. Cheng-Hua, U. Muhammad, L. Kuang-Lieh, *Science and Technology of Advanced Materials* **2015**, *16*, 054204; bM. D. Allendorf, V. Stavila, *CrystEngComm* **2015**, *17*, 229-246; cE. A. Dolgopolova, N. B. Shustova, *MRS Bull.* **2016**, *41*, 890-895; dI. Stassen, N. Burtch, A. Talin, P. Falcaro, M. Allendorf, R. Ameloot, *Chem. Soc. Rev.* **2017**, *46*, 3185-3241.
[5] aM. Usman, S. Mendiratta, K. L. Lu, *ChemElectroChem* **2015**, *2*, 786-788; bB. D. Hatton, K. Landskron, W. J. Hunks, M. R. Bennett, D. Shukaris, D. D. Perovic, G. A. Ozin, *Materials Today* **2006**, *9*, 22-31.
[6] B. Hoefflinger, *ITRS: The International Technology Roadmap for Semiconductors*, Springer, Berlin, Heidelberg, **2011**.
[7] *International Roadmap for Devices and Systems - More Moore White Paper*, **2016**.
[8] K. Zagorodniy, G. Seifert, H. Hermann, *Appl. Phys. Lett.* **2010**, *97*, 251905.
[9] aR. Warmbier, A. Quandt, G. Seifert, *J. Phys. Chem. C* **2014**, *118*, 11799-11805; bL. M. Yang, P. Ravindran, P. Vajeeston, M. Tilset, *Phys. Chem. Chem. Phys.* **2012**, *14*, 4713-4723.
[10] E. Redel, Z. B. Wang, S. Walheim, J. X. Liu, H. Gliemann, C. Woll, *Appl. Phys. Lett.* **2013**, *103*, 091903.
[11] aK. S. Park, Z. Ni, A. P. Cote, J. Y. Choi, R. Huang, F. J. Uribe-Romo, H. K. Chae, M. O'Keeffe, O. M. Yaghi, *Proc. Natl. Acad. Sci. U. S. A.* **2006**, *103*, 10186-10191; bS. Van Cleuvenbergen, I. Stassen, E. Gobechiya, Y. Zhang, K. Markey, D. E. De Vos, C. Kirschhock, B. Champagne, T. Verbiest, M. A. van der Veen, *Chem. Mater.* **2016**, *28*, 3203-3209.
[12] S. Eslava, L. P. Zhang, S. Esconjauregui, J. W. Yang, K. Vanstreels, M. R. Baklanov, E. Saiz, *Chem. Mater.* **2013**, *25*, 27-33.
[13] M. R. Ryder, Z. Zeng, Y. Sun, T. D. Bennett, I. Flyagina, K. Titov, E. M. Mahdi, B. Civalleri, C. S. Kelley, M. D. Frogley, G. Cinque, J. C. Tan, *arXiv:1802.06702 [cond-mat.mtrl-sci]*.
[14] aH. Deng, C. J. Doonan, H. Furukawa, R. B. Ferreira, J. Towne, C. B. Knobler, B. Wang, O. M. Yaghi, *Science* **2010**, *327*, 846-850; bM. Eddaoudi, J. Kim, N. Rosi, D. Vodak, J. Wachter, M. O'Keeffe, O. M. Yaghi, *Science* **2002**, *295*, 469-472.
[15] aC. K. Brozek, M. Dinca, *Chem. Sci.* **2012**, *3*, 2110-2113; bM. Fuentes-Cabrera, D. M. Nicholson, B. G. Sumpter, M. Widom, *J. Chem. Phys.* **2005**, *123*, 124713; cL.-M. Yang, P. Ravindran, P. Vajeeston, M. Tilset, *RSC Adv.* **2012**, *2*, 1618-1631.
[16] A. Walsh, K. T. Butler, C. H. Hendon, *MRS Bull.* **2016**, *41*, 870-876.
[17] aP. Canepa, K. Tan, Y. J. Du, H. B. Lu, Y. J. Chabal, T. Thonhauser, *J. Mater. Chem. A* **2015**, *3*, 986-995; bM. D. Allendorf, M. E. Foster, F. Leonard, V. Stavila, P. L. Feng, F. P. Doty, K. Leong, E. Y. Ma, S. R. Johnston, A. A. Talin, *J. Phys. Chem. Lett.* **2015**, *6*, 1182-1195; cA. De Vos, K. Hendrickx, P. Van Der Voort, V. Van Speybroeck, K. Lejaeghere, *Chem. Mater.* **2017**, *29*, 3006-3019.
[18] B. Civalleri, F. Napoli, Y. Noel, C. Roetti, R. Dovesi, *CrystEngComm* **2006**, *8*, 364-371.
[19] J. Gascon, M. D. Hernandez-Alonso, A. R. Almeida, G. P. van Klink, F. Kapteijn, G. Mul, *ChemSusChem* **2008**, *1*, 981-983.
[20] S. T. Meek, J. J. Perry, S. L. Teich-McGoldrick, J. A. Greathouse, M. D. Allendorf, *Cryst. Growth Des.* **2011**, *11*, 4309-4312.
[21] S. S. Kaye, A. Dailly, O. M. Yaghi, J. R. Long, *J. Am. Chem. Soc.* **2007**, *129*, 14176-14177.
[22] C. Hansch, A. Leo, R. W. Taft, *Chem. Rev. (Washington, DC, U. S.)* **1991**, *91*, 165-195.
[23] J. Long, S. Wang, Z. Ding, S. Wang, Y. Zhou, L. Huang, X. Wang, *Chem. Commun.* **2012**, *48*, 11656-11658.
[24] C. H. Hendon, D. Tiana, M. Fontecave, C. Sanchez, L. D'Arras, C. Sassoye, L. Rozes, C. Mellot-Draznieks, A. Walsh, *J. Am. Chem. Soc.* **2013**, *135*, 10942-10945.
[25] M. J. Katz, Z. J. Brown, Y. J. Colon, P. W. Siu, K. A. Scheidt, R. Q. Snurr, J. T. Hupp, O. K. Farha, *Chem. Commun.* **2013**, *49*, 9449-9451.

[26] aM. R. Ryder, B. Civalleri, J. C. Tan, *Phys. Chem. Chem. Phys.* **2016**, *18*, 9079-9087; bM. R. Ryder, B. Van de Voorde, B. Civalleri, T. D. Bennett, S. Mukhopadhyay, G. Cinque, F. Fernandez-Alonso, D. De Vos, S. Rudic, J. C. Tan, *Phys. Rev. Lett.* **2017**, *118*, 255502; cV. Guillerm, F. Ragon, M. Dan-Hardi, T. Devic, M. Vishnuvarthan, B. Campo, A. Vimont, G. Clet, Q. Yang, G. Maurin, G. Ferey, A. Vittadini, S. Gross, C. Serre, *Angew. Chem., Int. Ed.* **2012**, *51*, 9267-9271.

[27] R. J. Marshall, S. L. Griffin, C. Wilson, R. S. Forgan, *J. Am. Chem. Soc.* **2015**, *137*, 9527-9530.

[28] J. E. Mondloch, W. Bury, D. Fairen-Jimenez, S. Kwon, E. J. DeMarco, M. H. Weston, A. A. Sarjeant, S. T. Nguyen, P. C. Stair, R. Q. Snurr, O. K. Farha, J. T. Hupp, *J. Am. Chem. Soc.* **2013**, *135*, 10294-10297.

[29] P. D. Dietzel, B. Panella, M. Hirscher, R. Blom, H. Fjellvag, *Chem. Commun.* **2006**, 959-961.

[30] F. Bonino, S. Chavan, J. G. Vitillo, E. Groppo, G. Agostini, C. Lamberti, P. D. C. Dietzel, C. Prestipino, S. Bordiga, *Chem. Mater.* **2008**, *20*, 4957-4968.

[31] L. Valenzano, B. Civalleri, S. Chavan, S. Bordiga, M. H. Nilsen, S. Jakobsen, K. P. Lillerud, C. Lamberti, *Chem. Mater.* **2011**, *23*, 1700-1718.

[32] aS. L. Ling, B. Slater, *J. Phys. Chem. C* **2015**, *119*, 16667-16677; bK. Titov, Z. Zeng, M. R. Ryder, A. K. Chaudhari, B. Civalleri, C. S. Kelley, M. D. Frogley, G. Cinque, J. C. Tan, *J. Phys. Chem. Lett.* **2017**, *8*, 5035-5040.

[33] M. Sanchez-Andujar, S. Yanez-Vilar, B. Pato-Doldan, C. Gomez-Aguirre, S. Castro-Garcia, M. A. Senaris-Rodriguez, *J. Phys. Chem. C* **2012**, *116*, 13026-13032.

[34] aA. Buonaugurio, J. Graham, A. Buytendyk, K. H. Bowen, M. R. Ryder, Z. G. Keolopile, M. Haranczyk, M. Gutowski, *J. Chem. Phys.* **2014**, *140*, 221103; bZ. G. Keolopile, M. R. Ryder, B. Calzada, M. Gutowski, A. M. Buytendyk, J. D. Graham, K. H. Bowen, *Phys. Chem. Chem. Phys.* **2017**, *19*, 29760-29766.

[35] A. Pathak, G. R. Chiou, N. R. Gade, M. Usman, S. Mendiratta, T. T. Luo, T. W. Tseng, J. W. Chen, F. R. Chen, K. H. Chen, L. C. Chen, K. L. Lu, *ACS Appl. Mater. Interfaces* **2017**, *9*, 21872-21878.

[36] aC. G. Silva, A. Corma, H. Garcia, *J. Mater. Chem.* **2010**, *20*, 3141-3156; bM. Usman, S. Mendiratta, K. L. Lu, *Adv. Mater.* **2017**, *29*, 1605071-n/a.

[37] W. Volksen, R. D. Miller, G. Dubois, *Chem. Rev.* **2010**, *110*, 56-110.

[38] H. Wu, T. Yildirim, W. Zhou, *J. Phys. Chem. Lett.* **2013**, *4*, 925-930.

[39] aM. R. Ryder, J. C. Tan, *Dalton Trans.* **2016**, *45*, 4154-4161; bM. R. Ryder, B. Civalleri, G. Cinque, J. C. Tan, *CrystEngComm* **2016**, *18*, 4303-4312.

[40] C. Atzori, G. C. Shearer, L. Maschio, B. Civalleri, F. Bonino, C. Lamberti, S. Svelle, K. P. Lillerud, S. Bordiga, *J. Phys. Chem. C* **2017**, *121*, 9312-9324.

[41] aI. Buchan, M. R. Ryder, J. C. Tan, *Cryst. Growth Des.* **2015**, *15*, 1991-1999; bZ. G. Gu, S. C. Chen, W. Q. Fu, Q. Zheng, J. Zhang, *ACS Appl. Mater. Interfaces* **2017**, *9*, 7259-7264.

[42] aJ. M. Crowley, J. Tahir-Kheli, W. A. Goddard, 3rd, *J. Phys. Chem. Lett.* **2016**, *7*, 1198-1203; bP. Pernot, B. Civalleri, D. Presti, A. Savin, *J. Phys. Chem. A* **2015**, *119*, 5288-5304; cM. Ferrero, M. Rerat, R. Orlando, R. Dovesi, *J. Comput. Chem.* **2008**, *29*, 1450-1459; dM. Rerat, L. Maschio, B. Kirtman, B. Civalleri, R. Dovesi, *J. Chem. Theory Comput.* **2016**, *12*, 107-113; eM. Ferrero, B. Civalleri, M. Rerat, R. Orlando, R. Dovesi, *J. Chem. Phys.* **2009**, *131*, 214704.

[43] aA. D. Becke, *J. Chem. Phys.* **1993**, *98*, 5648-5652; bP. J. Stephens, F. J. Devlin, C. F. Chabalowski, M. J. Frisch, *J. Phys. Chem.* **1994**, *98*, 11623-11627; cC. T. Lee, W. T. Yang, R. G. Parr, *Phys. Rev. B* **1988**, *37*, 785-789.

[44] aB. Civalleri, C. M. Zicovich-Wilson, L. Valenzano, P. Ugliengo, *CrystEngComm* **2008**, *10*, 405-410; bS. Grimme, J. Antony, S. Ehrlich, H. Krieg, *J. Chem. Phys.* **2010**, *132*, 154104.

[45] aR. Dovesi, A. Erba, R. Orlando, C. M. Zicovich-Wilson, B. Civalleri, L. Maschio, M. Rerat, S. Casassa, J. Baima, S. Salustro, B. Kirtman, *WIREs Computational Molecular Science (2017) - Submitted* **2017**; bR. Dovesi, V. R. Saunders, C. Roetti, R. Orlando, C. M. Zicovich-Wilson, F. Pascale, B. Civalleri, K. Doll, N. M. Harrison, I. J. Bush, P. D'Arco, M. Llunell, M. Causà, Y. Noël, L. Maschio, A. Erba, M. Rerat, S. Casassa, *CRYSTAL17 User's Manual (University of Torino)* **2017**.

[46] aL. Maschio, B. Kirtman, M. Rerat, R. Orlando, R. Dovesi, *J. Chem. Phys.* **2013**, *139*, 164101; bL. Maschio, B. Kirtman, M. Rerat, R. Orlando, R. Dovesi, *J. Chem. Phys.* **2013**, *139*, 164102.

Entry for the Table of Contents (Please choose one layout)

Layout 1:

FULL PAPER

The work involves investigating a diverse range of metal-organic framework (MOFs) materials to understand how the different structural building blocks can affect the electronic properties and dielectric response. The analysis includes the contribution from the metals involved, the organic linkers and the symmetry and topology of the framework and makes suggestions for future work on low-κ dielectric MOFs.

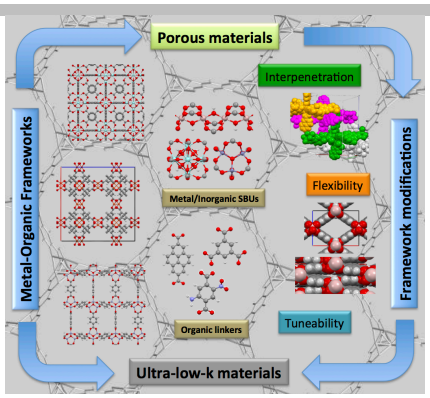

*Matthew R. Ryder, Lorenzo Donà, Jenny G. Vitillo, and Bartolomeo Civalleri**

Page No. – Page No.

Understanding and Controlling the Dielectric Response of Metal-Organic Frameworks